Design of 2-D Channel Estimation Filters for OFDM Systems

Ji-Woong Choi and Yong-Hwan Lee
School of Electrical Engineering and INMC, Seoul National University
Kwanak P. O. Box 34, Seoul, 151-744, Korea
e-mail: jwch@fruit.snu.ac.kr, ylee@snu.ac.kr

Abstract - **The performance of channel estimation can be improved by employing a channel estimation filter (CEF) that can adjust its bandwidth in response to the channel condition. For coherent OFDM receiver, we consider the use of two-dimensional (2-D) moving average (MA) FIR filter with a linear interpolation filter as the CEF that can provide good performance without requiring large implementation complexity. The optimum tap size of 2-D MA FIR CEF is analytically determined in terms of the pilot spacing, the channel spectrum and pilot signal to interference power ratio. The performance of the proposed channel estimator is evaluated by computer simulation.**

I. INTRODUCTION

Coherent detection is often employed in the orthogonal frequency division-multiplexing (OFDM) receiver to improve the detection performance. However, it requires accurate channel information. In order to obtain accurate channel estimate, the use of predetermined pilot symbols is widely applied in practice. In the OFDM system, pilot symbols are scattered in time and frequency domain to track time-varying and frequency selective channel characteristics. The channel impulse response (CIR) in the data region can be estimated by interpolating the CIR estimated using the scattered pilot symbols.

Two-dimensional (2-D) Wiener filters are considered as the optimum channel estimation filter (CEF) that minimizes the mean square error (MSE) of the channel estimate [1]. However, it may not be practical because of large implementation complexity. To reduce the implementation complexity, channel estimation can be performed independently in the time and frequency domain. The use of two 1-D Wiener filters in each domain can be considered instead of the use of a single 2-D Wiener filter because it can reduce the implementation complexity at the expense of a small performance loss [1]. However, it is still too complex to employ two 1-D Wiener filters in practice. As a result, a simple interpolator filter such as linear, Lagrange and Spline interpolation schemes is often employed for the CEF in practice [2,3]. However, since these CEFs use fixed parameters independent of the channel condition, they may result in severe performance degradation under certain channel condition.

In this paper, we consider the use of cascaded filter composed of linear interpolator (LI) and MA FIR filter as the CEF for simplicity of implementation without significant performance degradation. In the proposed scheme, the received signal is interpolated using linear interpolator to obtain instantaneous CIR, and then low-pass filtered using an MA FIR filter to suppress the excess noise. To the best knowledge of authors, few results have been reported on the analytic design of MA FIR CEF except some simulation results [4,5]. Moreover, they do not consider any interpolation. We analytically design 2-D MA FIR CEF by minimizing the MSE of the estimated CIR considering the effect of interpolation.

Following Introduction, Section Ⅱ describes an OFDM system. The optimum 2-D MA FIR CEF is analytically designed by minimizing the MSE of the estimated CIR in Section Ⅲ. The performance of the proposed scheme is verified in Section Ⅳ. Finally, conclusions are summarized in Section Ⅴ.

II. SYSTEM MODEL

In the OFDM transmitter, K data symbols at the n-th symbol time, $X[n,k]$, $k = 0, 1, 2,\ldots, K$-1, are converted into a time domain signal using the inverse fast Fourier transform (FFT). A cyclic prefix (CP) is inserted to preserve the orthogonality between the subcarriers and to eliminate the interference between the adjacent OFDM symbols. We assume that the pilot symbol is regularly inserted in a rectangular style, i.e., located apart by d_t and d_f symbols in the time and frequency grid, respectively.

We assume a wireless channel as

$$h(t,\tau) = \sum_{l=0}^{L-1} h_l(t)\delta(\tau - \tau_l) \tag{1.}$$

where L is the number of multipaths, $\delta(\cdot)$ is Kronecker delta function, τ_l and $h_l(t)$ are the delay and complex-valued CIR at time t of the l-th path, respectively. We assume that $h_l(t)$ has the same normalized correlation function $r_t(\triangle t)$ for all l. Then, the time-domain correlation of the l-th path CIR can be represented as

$$r_l(\triangle t) = E\{h_l(t+\triangle t)h_l^*(t)\} = \sigma_l^2 r_t(\triangle t) \tag{2.}$$

where $E\{X\}$ denotes the expectation of X, * denotes the complex conjugate and σ_l^2 denotes the average power of the l-th path. The frequency response of the CIR at time t can be written by

$$H(t,f) = \int_{-\infty}^{\infty} h(t,\tau)\mathrm{e}^{-j2\pi f\tau}d\tau = \sum_{l=0}^{L-1} h_l(t)\mathrm{e}^{-j2\pi f\tau_l}. \tag{3.}$$

Assuming $h_l(t)$ is statistically independent for each path with the normalized average path power (i.e., $\sum_{l=0}^{L-1}\sigma_l^2 = 1$), the correlation

0-7803-8939-5/05/$20.00 (C) 2005 IEEE

function of the frequency response can be represented as

$$r_H(\Delta t,\Delta f) = E\{H(t+\Delta t, f+\Delta f)H^*(t,f)\} = r_t(\Delta t)r_f(\Delta f) \quad (4.)$$

where $r_f(\Delta f) = \sum_{l=0}^{L-1} \sigma_l^2 \, e^{-j2\pi \Delta f \tau_l}$. In an OFDM symbol with symbol period T_s and subcarrier spacing Δf, the correlation function can be represented as $r_H[n,k] = r_t[n]r_f[k]$ where $r_t[n] = r_t(nT_s)$ and $r_f[k] = r_f(k\Delta f)$.

In the receiver, the CP is removed before the FFT process. Assuming ideal synchronization at the receiver, the received symbol of the *k*-th subcarrier at the *n*-th symbol time can be represented by

$$Y[n,k] = X[n,k]H[n,k] + Z[n,k] \quad (5.)$$

where $H[n,k]$ is the frequency response of the channel at the *k*-th subcarrier and the *n*-th symbol time, and $Z[n,k]$ is the background noise plus interference term, which can be approximated as zero mean additive white Gaussian noise (AWGN) with variance σ_Z^2.

III. OPTIMUM 2-D MA FIR CEF

The CIR can be estimated using the received pilot symbols as

$$\tilde{H}[n_p,k_p] = Y[n_p,k_p]/X[n_p,k_p] = H[n_p,k_p] + \tilde{Z}[n_p,k_p] \quad (6.)$$

where n_p and k_p denote the symbol and subcarrier index of the pilot symbol, respectively, and $\tilde{Z}[n_p,k_p]$ denotes the noise term. Assuming that $X[n_p,k_p] = 1$ without the loss of generality, $\tilde{Z}[n_p,k_p]$ can be assumed zero mean AWGN with variance σ_Z^2.

Note that the fading channel is band-limited to a maximum Doppler frequency f_d and has a maximum time delay τ_{L-1}. When $d_t f_d T_s \le 1/2$ and $d_f \tau_{L-1} \Delta f \le 1/2$, the CIR corresponding to the data symbol can be estimated by interpolating the CIR estimated using the scattered pilot symbols [7]. Since the impulse response of the ideal interpolator for a band-limited channel is a sinc function, the CIR can be represented as

$$\tilde{H}[n,k] = \sum_{p=-\infty}^{\infty} \sum_{q=-\infty}^{\infty} \tilde{H}_s[n+p,k+q] w_{id}[p,q] \quad (7.)$$

where $\tilde{H}_s[n,k]$ is equal to $\tilde{H}[n,k]$ at the pilot symbol and zero, otherwise, and $w_{id}[p,q]$ is the impulse response of an ideal 2-D brick-wall interpolator represented as

$$w_{id}[p,q] = \frac{\sin(\pi p/d_t)\sin(\pi q/d_f)}{(\pi p/d_t)(\pi q/d_f)}. \quad (8.)$$

Since it is impractical to realize $w_{id}[p,q]$ using a finite number of filter taps, we consider the use of an interpolator with simple structure. To obtain the CIR at the data symbol, the CIR estimated at the pilot symbol is linearly interpolated in the frequency domain and then in the time domain as

$$\tilde{H}[n_p,k_p+k] = \tilde{H}[n_p,k_p] + \frac{k}{d_f}(\tilde{H}[n_p,k_p+d_f] - \tilde{H}[n_p,k_p]),\ 0<k<d_f \quad (9.)$$

$$\tilde{H}[n_p+n,k] = \tilde{H}[n_p,k] + \frac{n}{d_t}(\tilde{H}[n_p+d_t,k] - \tilde{H}[n_p,k]),\ 0<n<d_t.$$

Since conventional interpolators including the linear interpolator use fixed parameters for simplicity of implementation, they may not provide desirable performance when the channel condition varies. To alleviate this problem, we consider the use of CEF composed of a linear interpolator and 2-D MA FIR filter, whose response is changeable by simply controlling the tap size. The excessive noise in the CIR estimate is removed using a 2-D MA FIR filter with N_t $(=2M_t+1)$ and N_f $(=2M_f+1)$ taps in the time and frequency domain, respectively, whose response is

$$\hat{H}[n,k] = \frac{1}{N_t N_f} \sum_{m_1=-M_t}^{M_t} \sum_{m_2=-M_f}^{M_f} \tilde{H}[n+m_1 d_t, k+m_2 d_f] \quad (10.)$$

where the tap size N_t and N_f are determined according to the channel condition.

It can be shown using (7) that

$$\begin{aligned}\hat{H}[n,k] &= \sum_{p=-\infty}^{\infty}\sum_{q=-\infty}^{\infty} \tilde{H}_s[n+p,k+q] w[p,q] \\ &= H[n,k] + \sum_{p=-\infty}^{\infty}\sum_{q=-\infty}^{\infty} \{H_s[n+p,k+q](w[p,q] - w_{id}[p,q])\} \\ &\quad + \sum_{p=-\infty}^{\infty}\sum_{q=-\infty}^{\infty} \{\tilde{Z}_s[n+p,k+q] w[p,q]\}\end{aligned} \quad (11.)$$

where $\tilde{Z}_s[n,k]$ is equal to $\tilde{Z}[n,k]$ at the pilot symbol and zero, otherwise, $w[p,q]$ denotes the overall impulse response of the proposed CEF (i.e., the cascaded linear interpolator and MA FIR filter). Note that $\hat{H}[n,k]$ is composed of perfect CIR, self-distorted signal due to the use of non-ideal interpolator and interference signal.

Defining the MSE of the CIR estimate by σ_e^2, it can be represented as

$$\begin{aligned}\sigma_e^2 &= E\{|\hat{H}[n,k] - H[n,k]|^2\} \\ &= \frac{1}{(2\pi)^2} \int_{-\pi}^{\pi}\int_{-\pi}^{\pi} S_{H_s}(w_1,w_2)|W_e(w_1,w_2)|^2 dw_1 dw_2 + \frac{\sigma_Z^2}{N_t N_f}\end{aligned} \quad (12.)$$

where $S_{H_s}(w_1,w_2)$ is the sampled $S_H(w_1,w_2)$ [6],

$$S_{H_s}(w_1,w_2) = \frac{1}{(d_t d_f)^2} \sum_{n=0}^{d_f-1}\sum_{k=0}^{d_t-1} S_H(w_1 - \frac{2\pi}{d_t}n, w_2 - \frac{2\pi}{d_f}k). \quad (13.)$$

Here, $S_H(w_1,w_2)$ is the 2-D Fourier transform (FT) of $r_H[n,k]$

$$\begin{aligned}S_H(w_1,w_2) &\equiv \sum_{n=-\infty}^{\infty}\sum_{k=-\infty}^{\infty} r_H[n,k] e^{-j(w_1 n + w_2 k)} \\ &= \sum_{n=-\infty}^{\infty} r_t[n] e^{-jw_1 n} \cdot \sum_{k=-\infty}^{\infty} r_f[k] e^{-jw_2 k} \\ &= S_{H_1}(w_1) S_{H_2}(w_2)\end{aligned} \quad (14.)$$

where $S_{H_1}(w_1)$ and $S_{H_2}(w_2)$ are the FT of $r_t[n]$ and $r_f[k]$, respectively. Letting $w_e[p,q] = w[p,q] - w_{id}[p,q]$, the 2-D FT of $w_e[p,q]$ can be represented as

$$W_e(w_1,w_2) = \begin{cases} W(w_1,w_2) - d_t d_f, & |w_1| \le \pi/d_t \text{ and } |w_2| \le \pi/d_f \\ W(w_1,w_2), & \text{otherwise} \end{cases} \quad (15.)$$

where $W(w_1,w_2)$ is the 2-D FT of $w[p,q]$ represented as [7]

$$W(w_1,w_2) = \frac{1}{d_t d_f}\left(\frac{\sin(w_1 d_t/2)}{\sin(w_1/2)}\frac{\sin(w_2 d_f/2)}{\sin(w_2/2)}\right)^2 \cdot \frac{1}{N_t N_f}\left(\frac{\sin(w_1 d_t N_t/2)}{\sin(w_1 d_t/2)}\frac{\sin(w_2 d_f N_f/2)}{\sin(w_2 d_f/2)}\right). \quad (16.)$$

Neglecting the out-of-passband signal and using a Taylor series approximation of $|W_e(w_1,w_2)|^2$ for $d_t,\ d_f \ge 2$, the MSE can be approximated as

$$\begin{aligned} \sigma_e^2 &\approx \frac{1}{(2\pi)^2}\int_{-\pi/d_f}^{\pi/d_f}\int_{-\pi/d_t}^{\pi/d_t} S_{H_s}(w_1,w_2)\left(c_0 w_1^2 w_2^2 + c_1 w_1^4 + c_2 w_2^4\right)dw_1\,dw_2 + \frac{\sigma_Z^2}{N_t N_f} \\ &= \frac{1}{(d_t d_f)^2 (2\pi)^2}\int_{-\pi}^{\pi}\int_{-\pi}^{\pi} S_{H_1}(w_1) S_{H_2}(w_2)\left(c_0 w_1^2 w_2^2 + c_1 w_1^4 + c_2 w_2^4\right)dw_1\,dw_2 + \frac{\sigma_Z^2}{N_t N_f} \\ &= \frac{1}{(d_t d_f)^2}\left(c_0 \bar{w}_1^{(2)}\bar{w}_2^{(2)} + c_1 \bar{w}_1^{(4)} + c_2 \bar{w}_2^{(4)}\right) + \frac{\sigma_Z^2}{N_t N_f} \end{aligned} \quad (17.)$$

where $\bar{w}_1^{(n)}$ and $\bar{w}_2^{(n)}$ are respectively the *n*-th order moment of the Doppler spectrum and power delay profile

$$\bar{w}_1^{(n)} = \frac{1}{2\pi}\int_{-\pi}^{\pi} w_1^n S_{H_1}(w_1)dw_1$$

$$\bar{w}_2^{(n)} = \frac{1}{2\pi}\int_{-\pi}^{\pi} w_2^n S_{H_2}(w_2)dw_2 \quad (18.)$$

and c_0, c_1 and c_2 are the coefficient of the approximated polynomial represented as

$$\begin{aligned} c_0 &= d_t^2 d_f^2 (d_t^2 N_t^2 - 2)(d_f^2 N_f^2 - 2)/288 \approx d_t^2 d_f^2 (d_t^2 N_t^2)(d_f^2 N_f^2)/288 \\ c_1 &= d_t^2 d_f^2 (d_t^2 N_t^2 - 2)^2/576 \approx d_t^2 d_f^2 (d_t^2 N_t^2)^2/576 \\ c_2 &= d_t^2 d_f^2 (d_f^2 N_f^2 - 2)^2/576 \approx d_t^2 d_f^2 (d_f^2 N_f^2)^2/576. \end{aligned} \quad (19.)$$

Thus, it can be seen that

$$\begin{aligned} \sigma_e^2 &\approx \frac{1}{576}\left(2\bar{w}_1^{(2)}\bar{w}_2^{(2)} d_t^2 d_f^2 N_t^2 N_f^2 + \bar{w}_1^{(4)} d_t^4 N_t^4 + \bar{w}_2^{(4)} d_f^4 N_f^4\right) + \frac{\sigma_Z^2}{N_t N_f} \\ &\ge \frac{1}{576}\left(2\bar{w}_1^{(2)}\bar{w}_2^{(2)} d_t^2 d_f^2 N_t^2 N_f^2 + 2\sqrt{\bar{w}_1^{(4)}\bar{w}_2^{(4)}}\, d_t^2 d_f^2 N_t^2 N_f^2\right) + \frac{\sigma_Z^2}{N_t N_f} \\ &= \frac{(d_t d_f)^2 (N_t N_f)^2}{288}\left(\bar{w}_1^{(2)}\bar{w}_2^{(2)} + \sqrt{\bar{w}_1^{(4)}\bar{w}_2^{(4)}}\right) + \frac{\sigma_Z^2}{N_t N_f} \end{aligned} \quad (20.)$$

where the equality holds when

$$\bar{w}_1^{(4)} d_t^4 N_t^4 = \bar{w}_2^{(4)} d_f^4 N_f^4. \quad (21.)$$

Assuming that $N_t N_f$ is a continuous parameter for ease of analytic design, the optimum $N_t N_f$ can uniquely be determined by solving

$$\frac{\partial \sigma_e^2}{\partial (N_t N_f)} = 0. \quad (22.)$$

Thus, the MSE becomes minimum, i.e.,

$$\begin{aligned} \sigma_{e,\min}^2 &= \frac{1.5\sigma_Z^2}{\left(N_t N_f\right)_{opt}} \\ &= (3/128)^{1/3}(d_t d_f)^{2/3}(\sigma_Z^2)^{2/3}\left(\bar{w}_1^{(2)}\bar{w}_2^{(2)} + \sqrt{\bar{w}_1^{(4)}\bar{w}_2^{(4)}}\right)^{1/3} \end{aligned} \quad (23.)$$

when

$$\left(N_t N_f\right)_{opt} = \frac{1}{\left(d_t d_f\right)^{2/3}}\left(\frac{144\sigma_Z^2}{\left(\bar{w}_1^{(2)}\bar{w}_2^{(2)} + \sqrt{\bar{w}_1^{(4)}\bar{w}_2^{(4)}}\right)}\right)^{1/3}. \quad (24.)$$

It can be seen that the minimum MSE increases as the pilot spacing, interference power and moments of the channel spectrum increase.

Using (21) and (24), the optimum tap size $\hat{N}_t$ and $\hat{N}_f$ can be determined by

$$\begin{aligned} \hat{N}_t &= \frac{\left(d_t d_f\right)^{1/6}}{d_t}\left(\frac{\bar{w}_2^{(4)}}{\bar{w}_1^{(4)}}\right)^{1/8}\left(\frac{144\sigma_Z^2}{\left(\bar{w}_1^{(2)}\bar{w}_2^{(2)} + \sqrt{\bar{w}_1^{(4)}\bar{w}_2^{(4)}}\right)}\right)^{1/6} \\ \hat{N}_f &= \frac{\left(d_t d_f\right)^{1/6}}{d_f}\left(\frac{\bar{w}_2^{(4)}}{\bar{w}_1^{(4)}}\right)^{-1/8}\left(\frac{144\sigma_Z^2}{\left(\bar{w}_1^{(2)}\bar{w}_2^{(2)} + \sqrt{\bar{w}_1^{(4)}\bar{w}_2^{(4)}}\right)}\right)^{1/6}. \end{aligned} \quad (25.)$$

It can be seen that the 2-D MA FIR CEF should be designed considering the signal to interference power ratio (SIR) ($=1/\sigma_z^2$), pilot spacing, and the second- and fourth-order moment of the Doppler spectrum and power-delay profile of the channel. It can also be seen that the lower SIR, the larger the tap size is required to suppress the interference. As the moments of w_1 or w_2 decrease (i.e., the channel has small Doppler frequency or delay spread), it requires the increase of the tap size, and vice versa. Since the SIR and moment information of the channel can be estimated with low complexity by exploiting the autocorrelation property of the pilot signal as in [10], the proposed scheme can be employed in practice. Note also that although the analysis is performed considering the use of linear interpolator and MA FIR filter, similar derivation can be easily applied to the use of any other types of CEF by changing only $W(w_1,w_2)$ in (16).

IV. PERFORMANCE EVALUATION

To investigate the effect of channel estimation on the receiver performance, the performance is evaluated in terms of the MSE of the CIR estimate and bit error rate (BER) of the receiver. The simulation condition is summarized in Table 1 [8]. For performance comparison, we also consider the performance of 2-D Wiener CEF. The tap size of 2-D Wiener CEF is set to 80 and 20 in the time and frequency domain, respectively, since the use of additional taps provides marginal performance improvement. To compare the

performance of non-adaptive channel estimators, we consider the use of CEF composed of a linear interpolator and fixed 2-D MA FIR CEF. When fixed 2-D MA FIR CEF is employed, the tap size should be small in order to operate well under severe channel condition, i.e., fast time variant and severe frequency selective channel, as well as under mild condition. Thus, we consider the fixed MA FIR CEF whose tap size is $N_t = 5$ and $N_f = 3$ assuming $L_{\max} = 64$, $f_{d,\max} = 1342.6$ Hz and SIR = 20 dB. We also consider the use of the linear interpolator with no MA FIR CEF to know the effect of the MA FIR CEF.

Fig. 1 depicts the MSE of the CIR estimate under fading channel having a classic spectrum (i.e., Jake's model [9]) with an exponential power delay profile. We neglect the edge effect at both ends of the frequency band for simplicity of comparison. Note that the tap size of the optimum MA FIR CEF designed by (25) is depicted in Fig. 1. It can be seen that the optimum MA FIR CEF provides receiver performance slightly worse than that of the Wiener CEF. It can be seen that the performance difference between the optimum MA FIR CEF and Wiener CEF increases as the SIR increases. This is mainly due to the fact that the MA FIR CEF uses decreased tap size (from (80,20) at SIR = 0dB to (31,8) at SIR = 25dB), while the Wiener CEF use a fixed large tap size (80,20). For example, when the tap size of the Wiener CEF is reduced from (80,20) to (40,20), the performance degradation is noticeably degraded. As a result, when the SIR is low, the Wiener CEF may results in the receiver performance worse than the optimum MA FIR CEF unless it uses sufficiently large tap size. On the other hand, the linear interpolator with no MA FIR CEF or fixed MA FIR CEF provides the MSE significantly larger than the Wiener CEF.

Fig. 2 and 3 depict the BER performance with the use of convolutional coding in slow and fast fading channels, respectively. Note that the BER performance with $L = 32$ is better than that with $L = 2$ due to the effect of increased frequency diversity. It can be seen that the optimum MA FIR CEF can provide BER performance similar to the Wiener CEF in most of channel condition. However, the linear interpolator with no MA FIR CEF or fixed MA FIR CEF provides significantly degraded performance, particularly when the channel has a small number of multipaths and/or the mobility is slow. This is mainly due to the fact that the fixed parameters are not matched to the channel condition.

In order to compare the complexity, we consider the required number of multiplications. The proposed scheme requires $(d_f - 1)/d_t + (d_t - 1) + 1$ multiplications per symbol while single 2-D Wiener CEF and two 1-D Wiener CEFs require $N_t N_f$ and $N_f / d_t + N_t$ multiplications, respectively. For example, 3.67 multiplications are requisite for the proposed scheme while 1600 and 86.67 ones are required for 2-D and 1-D Wiener CEFs, respectively, when $N_t = 80$, $N_f = 20$, $d_t = 3$ and $d_f = 3$. Thus, it is quite practical to employ the proposed CEF considering the implementation complexity and the receiver performance.

V. CONCLUSIONS

In this paper, we have considered the use of 2-D MA FIR filters with linear interpolation as the CEF for ease of design and implementation. For a given channel condition, we analytically derive the optimum tap size which can be determined in terms of the pilot spacing and channel condition parameters including the SIR and moments of the Doppler spectrum and power delay profile. Simulation results show that the proposed MA FIR CEF can provide the BER performance similar to the Wiener CEF, while significantly reducing the implementation complexity. Thus, the use of proposed scheme can be a good practical choice as the CEF in the OFDM system considering the implementation complexity and performance.

RERFERENCE

[1] P. Hoeher, S. Kaiser and P. Robertson, "Two-dimensional pilot-symbol aided channel estimation by Wiener filtering," *Proc. ICASSP'97*, pp. 1845-1848, Apr. 1997.

[2] S. Coleri, M. Ergen, A. Puri and A. Bahai, "Channel estimation techniques based on pilot arrangement in OFDM systems," *IEEE Trans. Broadcasting*, vol. 48, no. 3, Sept. 2002.

[3] K. F. Lee and D. B. Williams, "Pilot-symbol-assisted channel estimation for space-time coded OFDM systems," *EURASIP J. Applied Signal Process.*, vol. 2002, no. 5, pp. 507-516, May 2002.

[4] M. Benthin and K. Kammeyer, "Influence of channel estimation on the performance of a coherent DS-CDMA System," *IEEE Trans. Veh. Technol.*, vol. 46, no. 2, pp. 262-268, May 1997.

[5] H. Atarashi, S. Abeta and M. Sawahashi, "Performance evaluation of coherent high-speed TD-OFCDM broadband packet wireless access in forward link employing multi-level modulation and hybrid ARQ," *IEICE Trans. Fundamentals*, vol. E84-A, no. 7, pp. 1670-1680, July 2001.

[6] D. E. Dudgeon and R. M. Mersereau, *Multidimensional Digital Signal Processing*, Prentice Hall, 1984.

[7] A. V. Oppenheim and R. W. Schafer, *Discrete-time signal processing*, second edition, Prentice Hall, 1999.

[8] H. Atarashi, S. Abeta and M. Sawahashi, "Variable spreading factor-orthogonal frequency and code division multiplexing (VSF-OFCDM) for broadband packet wireless access," *IEICE Trans. Commun.*, vol. E86-B, no. 1, pp. 291-299, Jan. 2003.

[9] W. C. Jakes, *Microwave mobile communications*, John Wiley and Sons, 1974.

[10] J.-W. Choi, *Design of adaptive OFDM wireless transceivers*, Ph. D. dissertation, Seoul National University, Aug. 2004.

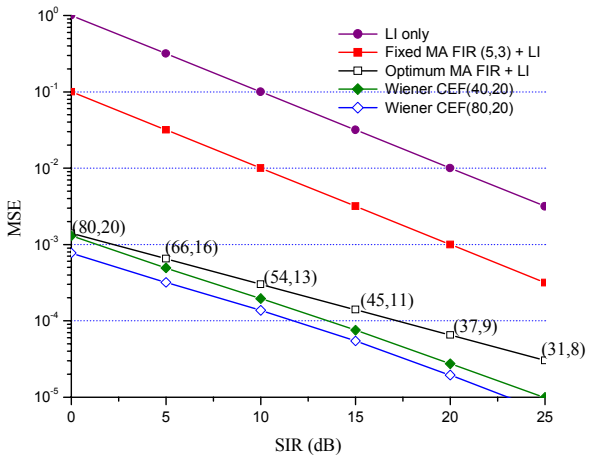

Fig. 1. MSE performance when L= 2 and $f_d T_S$ = 0.00043 (10 km/h).

Table 1. Simulation condition.

Parameters	Values
Total bandwidth	80 MHz
Symbol duration	6.4 μs (+1.6 μs: guard interval)
FFT size	512
Subcarrier spacing	156.3 kHz
Pilot occupation	11.1 % (d_t =3, d_f =3)
Carrier frequency	5.8 GHz
Allowable maximum Doppler frequency	$f_{d,\max}$ = 1342.6 Hz (250 km/h)
Channel coding	Convolutional coding (Code rate=1/2, constraint length=9)
Modulation	QPSK
Channel	Rayleigh (Classic spectrum)
Power delay profile	Exponential (Decaying factor:5, 12.5ns equi-spaced)

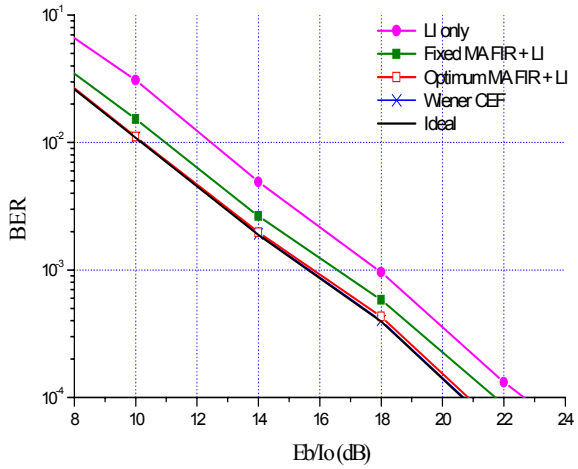

(a) L=2

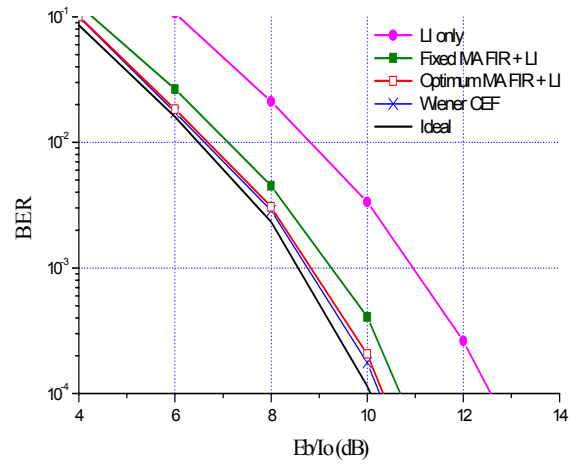

(b) L=32

Fig. 2. BER performance when $f_d T_S$ = 0.00043 (10 km/h).

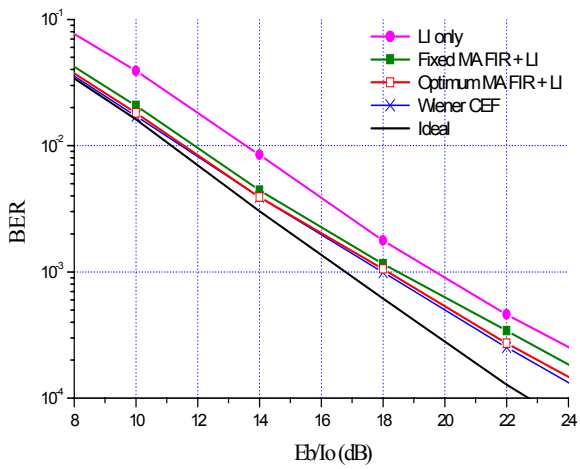

(a) L=2

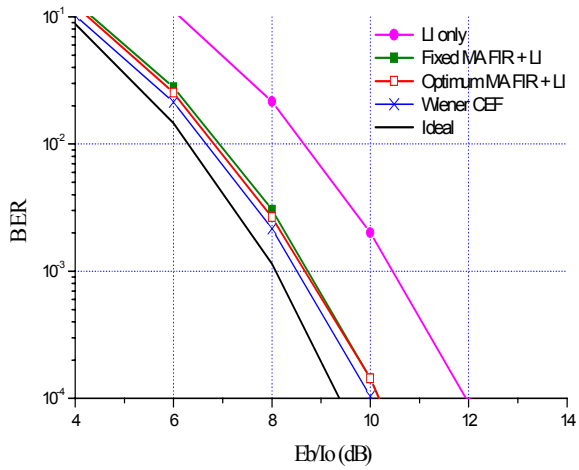

(b) L=32

Fig. 3. BER performance when $f_d T_S$ = 0.0107 (250 km/h).